fortune Journals

Research Article

INTERNATIONAL
JOURNAL OF APPLIED BIOLOGY AND PHARMACEUTICAL TECHNOLOGY
ISSN: 0976-4550

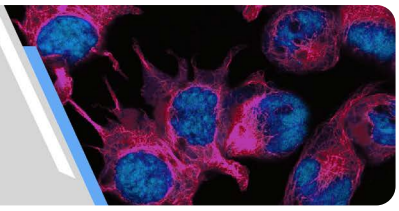

New Metal-Carbon Heterostructures with Enhanced Relaxivity for MRI Applications

Vasily T Lebedev*[,1], Natalia P Yevlampieva[1], Maria V Popova[2], Mikhail A Vovk[1], Alexander V Shvidchenko[3], Biligma B Tudupova[3], Victor I Kuular[3]

Abstract

Heterostructures of fullerenols $Fe@C_{60}(OH)_{30}$, $Gd@C_{82}(OH)_{30}$, $Ho@C_{82}(OH)_{40}$ with 4f and 3d metals in carbon cages and detonation nanodiamonds have been synthesized for prospect applications in Magnetic Resonance Imaging, Photodynamic Therapy and Nuclear Medicine using radioactive isotopes. We used fullerenols obtained by hydroxylation of endofullerenes produced in electric arc and nanodiamonds DNDZ+ and DNDZ- (size ~ 4.5 nm, positive (negative) potential in water 30-70 mV), chemically purified and annealed in hydrogen (air) flows. In aqueous mixtures with diamonds, fullerenols via hydroxyls formed hydrogen bonds with the H, OH, COOH groups on diamond surface. The association of components was facilitated by hydrophobic interactions and electrostatic attraction if DNDZ+ diamonds with positive surface charge were used. Aqueous dispersions of the complexes with magnetic atoms (Gd, Ho, Fe) at the temperature of 298 K have been studied by NMR. We corrected the measured reciprocal times of proton spin longitudinal and transverse relaxation ($1/T_1$,$1/T_2$) to water contributions ($1/T_{1,2W}$) and defined the relaxation rates $r_{1,2}= [1/T_{1,2} - 1/T_{1,2W}]$. Normalizing them to metal concentrations (C_M) we got the differential relaxivities $\Delta r = (r_2-r_1)/C_M$ showing the MRI contrast abilities of substances. The complexes $Gd@C_{82}(OH)_X$+DNDZ-, $Ho@C_{82}(OH)_X$+DNDZ+ with Δr ~20 $s^{-1}mM^{-1}$ and Δr ~ 24 $s^{-1}mM^{-1}$ are for ~ 6 and ~ 3 times and the complexes $Fe@C_{60}(OH)_X$+DNDZ- with Δr ~ 52 $s^{-1}mM^{-1}$ for ~ 12 times more efficient than pure fullerenols. Thus, the diamond platforms allowed greatly enhance the relaxivity of fullerenols.

Keywords: endofullerene, nanodiamond, proton spin relaxation, contrast agent, magnetic resonance imaging

Introduction

Development of composite nanostructures for theranostics is aimed at expanding the diagnostic capabilities of drugs when combined with a therapeutic effect [1-3]. This requires searching for opportunities to maximize both diagnostic and therapeutic factors by combining the beneficial properties of selected components and ensuring targeted delivery of drugs that should be placed on appropriate platforms (quantum dots, iron oxide nanoparticles, gold shell-type structures), capable, among other things, of stimulating the activity of drugs [1]. Metal oxides, metal-organic frameworks (e.g. of gold and silicon), and nanoparticles doped with lanthanides are used to solve these problems [4]. Additives with special properties (optical, fluorescent, magnetic, radioactive) being necessary for visualizing the resulting nanoparticles are introduced into porous platforms together with therapeutic agents [1-3]. Such a typic example is a construction of magnetic nanoparticles with surface modification or using biogenic synthesis for numerous applications (drug delivery, gene

Affiliation:

[1]Petersburg Nuclear Physics Institute named by B.P. Konstantinov, National Research Center Kurchatov Institute, Gatchina, Leningrad region, Russia

[2]St. Petersburg State University, St. Petersburg, Russia

[3]Ioffe Institute, St. Petersburg, Russia

***Corresponding Authors:**
Vasily T Lebedev, Petersburg Nuclear Physics Institute named by B.P. Konstantinov, National Research Center Kurchatov Institute, Gatchina, Leningrad region, Russia.

Citation: Vasily T Lebedev, Natalia P Yevlampieva, Maria V Popova, Mikhail A Vovk, Alexander V Shvidchenko, Biligma B Tudupova, Victor I Kuular. New Metal-Carbon Heterostructures with Enhanced Relaxivity for MRI Applications. International Journal of Applied Biology and Pharmaceutical Technology. 16 (2025): 02-11.

Received: August 01, 2025
Accepted: August 05, 2025
Published: August 12, 2025

Lebedev VT, et al., Int J Appl Biol Pharm 2025
DOI:10.26502/ijabpt.202135

chemo-, photo- and photodynamic therapy, hyperthermia, photoacoustics and ultrasound imaging, bioseparation, tissue engineering) [5]. These functional objects are studied for biocompatibility, toxicity, environmental safety [5] and various physical and chemical properties using IR, Raman, photoelectron, optical spectroscopy of UV and visible light absorption, magnetometry, electron microscopy, X-ray diffraction and scattering, dynamic light scattering for the analysis of the structure and particle size distributions, thermal gravimetry for determining the mass and composition of the organic coating of the surface of inorganic particles [6].

When selecting platforms for medicine, one has to choose the nanodiamonds as especially attractive entities due to the unique chemical-mechanical properties of the crystal faces for the design of therapeutic combinations in the interests of personalized medicine [7]. For targeted delivery and overcoming cellular resistance to commercial drugs, methods for associating drugs with nanodiamonds and their hybrids with nanoporous silicon are being developed since nanodiamonds may serve as good selective drug carriers due to their tiny dimensions, biocompatibility, and ability to avoid recognition by the immune system, when penetrating into the cytoplasm of diseased cells for targeted controlled release of chemotherapeutic agents with minimal nonspecific binding and toxicity to normal cells [8]. Small-sized detonation nanodiamonds (DND, 4-5 nm) with a large specific surface area (~400 m^2/g) are in demand for binding and delivering drugs in theranostics, since they are non-toxic and inert in chemically aggressive environments, and can serve as markers with appropriate surface modification [9,10]. In this regard, the effective methods have been developed for grafting various functional groups (H, OH, COOH, SO_3H, F) to diamonds to regulate their chemical activity, hydrophilic (hydrophobic) properties and electrical potential (positive, negative) which ensures the stability of diamond hydrosols (concentrations ≤ 1% wt.) and hydrogels (5-7% wt.) studied by viscometry, light and neutron scattering [11-14].

The chemical composition and the charge state of the surface of diamonds as regulated by grafted groups are important for these particles' selective interaction, contact and penetration into biological cells (microorganisms) [15]. Specially designed functional groups on the diamond surface are required for immobilization of medicinal (diagnostic) preparations by means of ionic and hydrogen bonds, hydrophobic interactions [16,17]. In this way, heterostructures can be created for theranostics, for example, by attaching fullerenes (endofullerenes) to diamonds [17,18] as far as these molecules are the strongest photosensitizers and molecular magnets, thereby obtaining therapeutic preparations serving also as the contrast agents to combine photodynamic therapy (PDT) and magnetic resonance imaging (MRI) [19,20]. The aim of our work was to develop the methods for synthesizing heterostructures by coupling endohedral fullerenols with 3d and 4f elements to nanodiamonds with following studies of magnetic relaxation properties of new substances in water comparative to free fullerenols.

Experimental

Sample Preparation and Attestation

As a magnetic component we used water-soluble fullerenols $Fe@C_{60}(OH)_{30}$, $Gd@C_{82}(OH)_{30}$, $Ho@C_{82}(OH)_{40}$ encapsulating 3d or 4f metal atoms inside carbon cages with grafted hydroxyls. Such molecules were associated with DND particles to prepare the heterostructures for promising applications in MRI, PDT and nuclear medicine employing radioactive isotopes [21, 22]. To obtain the DND component, diamond agglomerates were extracted from the carbon batch after detonation synthesis, milled and etched in acids to clean crystalline surface from graphene fragments [23,24]. The desirable chemical composition of diamond surface was formed by grafting to it various functional groups (H, OH; COOH) to impart the particles a positive (negative) potential (30-70 mV in aqueous environment) by annealing in flow of hydrogen (500°C) or air (450°C) [24-26]. The prepared particles DNDZ+, DNDZ- tested by TEM (Fig.1, Libra 200 FE electron microscope) have had a mean size 4.5 nm according to the size distribution found from dynamic light scattering measurements in their stable hydrosols, which also transformed into thixotropic hydrogels upon concentration (5-7 wt.%) [13,14]. Fig.1 illustrates well the DNDZ+ particles aggregation in dried hydrosol.

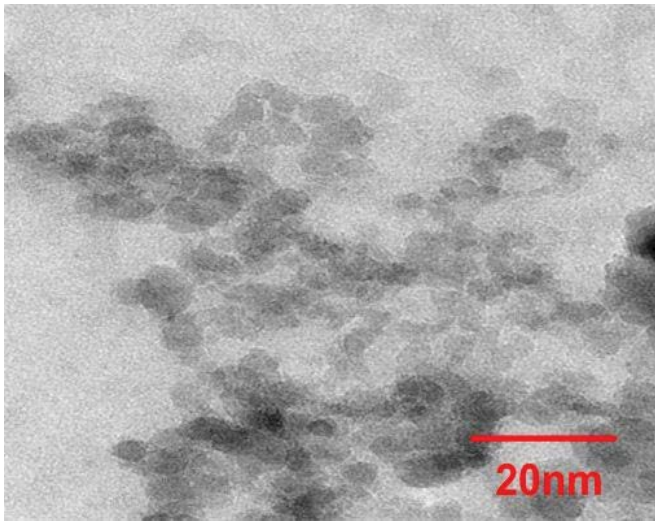

Figure 1: TEM pattern for DNDZ+ diamonds and their aggregates in dried hydrosol.

Citation: Vasily T Lebedev, Natalia P Yevlampieva, Maria V Popova, Mikhail A Vovk, Alexander V Shvidchenko, Biligma B Tudupova, Victor I Kuular. New Metal-Carbon Heterostructures with Enhanced Relaxivity for MRI Applications. International Journal of Applied Biology and Pharmaceutical Technology. 16 (2025): 02-11.

Lebedev VT, et al., Int J Appl Biol Pharm 2025
DOI:10.26502/ijabpt.202135

To prepare the molecular component, the endofullerenes (EF) with different metals, Fe@C_{60}, Gd@C_{82} and Ho@C_{82}, were synthesized, purified and finally hydroxylated when water-soluble fullerenols (HEF), Fe@$C_{60}(OH)_{30}$, Gd@$C_{82}(OH)_{30}$ and Ho@$C_{82}(OH)_{40}$, were produced [21,22]. For the production of EF with lanthanides, Gd@C_{82} and Ho@C_{82}, we used electric arc spraying of lanthanide oxide-filled graphite rods [27]. The resulting soot was extracted with o-xylene in a Soxhlet apparatus to remove empty fullerenes. From the residue the EF molecules were isolated with dimethylformamide [27]. In following treatment at the first stage there were attached ~10 hydroxyls to EF molecules, at the second stage the high degree of hydroxylation of 30 or 40 for the molecules Gd@$C_{82}(OH)_{30}$ and Ho@$C_{82}(OH)_{40}$ was achieved [21]. The synthesis of Ln@$C_{82}(OH)_X$ molecules was confirmed by IR spectra showed the characteristic lines (wave numbers of 3445 cm^{-1}, 1395 cm^{-1} for νO-H and δO-H vibrations), the amounts of OH groups in the molecules were found from gravimetry measurements [21]. In similar way there were obtained the EF with iron then converted into water-soluble Fe@$C_{60}(OH)_{30}$ derivative [22]. For all fullerenols the endohedral structure with metal atoms in the M^{3+} state due to electron transfer to carbon shells has been established by X-ray diffraction, EXAFS, X-ray fluorescence and gamma resonance spectroscopy [27-29].

Binary complexes HEF+DNDZ-, HEF+DNDZ+ have been prepared by mixing components dispersed in deionized water under mechanical and ultrasonic stirring, when hydrogen bonds were formed between them through functional groups and also the contacts of components may arise preferably between hydrophobic spots on their surfaces. Complexing was favored also by Coulomb attractions between positively charged diamonds DNDZ+ and electronegative fullerenols, while the association of DNDZ-particles having negative potential with like-charged fullerenols was weakened due to mutual repulsion. However, very polar aqueous medium reduced by two orders of magnitude all electrostatic interactions. Under such conditions, the observed specificity of magneto-relaxation properties of the heterostructures (Tab.1) should be mainly influenced by complicated cross-interactions of fullerenols and diamonds taking into account that the particles of both components as along trend to be self-organized into chain-like fractal entities in aqueous media [29-31].

In further NMR studies at the temperature of 298 K we tested the aqueous dispersions of components and complexes of DNDZ± with the fullerenols containing different magnetic atoms (Gd, Ho, Fe) (Tab.1). The results were compared with the data for the solvent being deionized water at the same conditions. Such water contained a minor O_2 impurity (0.54 mg/l) that is only ~ 6 % regarding to the amount corresponding to its solubility [32-34]. Meanwhile, this caused a decrease of in measured relaxation times for the solvent (Tab.1) comparative to these ones for completely pure water ($T_1 \approx$ 1.68 s и $T_2 \approx$ 1.05 s) [32]. However, this inconsistency did not influence the final results when we found the relaxivities for magnetic ions since the contribution of solvent was subtracted from the reciprocal relaxation times in following data treatment.

Table 1: Composition of the samples, molar concentrations of magnetic ions (C_M), times of longitudinal (T_1) and transverse (T_2) spin relaxation of protons, relaxivities (Δr) at ambient temperature (298 K)

№	Components, mg/ml		C_M, mM	T_1*, s	T_2*, s	Δr, $s^{-1}mM^{-1}$
1	DNDZ+, 3.0	-	-	2.72	0.732	-
2	DNDZ-, 3.2	-	-	2.59	0.827	-
3	DNDZ-, 3.2	Gd@$C_{82}(OH)_{30}$, 1.5	0.909	0.774	0.051	19.67±0.01
4	DNDZ+, 3.0	Gd@$C_{82}(OH)_{30}$, 1.5	0.909	0.947	0.084	11.46±0.01
5	-	Gd@$C_{82}(OH)_{30}$, 3.0	1.817	0.073	0.049	3.45±0.01
6	H_2O	-	-	3.38	1.37	-
7	-	Ho@$C_{82}(OH)_{40}$, 3.0	1.64	0.571	0.073	7.02±0.01
8	DNDZ-, 3.2	Ho@$C_{82}(OH)_{40}$,1.5	0.82	1.06	0.074	14.80±0.01
9	DNDZ+, 3.0	Ho@$C_{82}(OH)_{40}$, 1.5	0.82	1.02	0.048	23.68±0.01
10	-	Fe@$C_{60}(OH)_{30}$, 3.3	2.566	0.288	0.067	4.29±0.01
11	DNDZ-, 3.2	Fe@$C_{60}(OH)_{30}$, 1.6	1.244	0.159	0.014	52.01±0.08
12	DNDZ+, 3.0	Fe@$C_{60}(OH)_{30}$, 1.6	1.244	1.12	0.05	15.01±0.01

*T_1,T_2 measured with a high accuracy, errors ~ $2 \cdot 10^{-5}$ s.

Citation: Vasily T Lebedev, Natalia P Yevlampieva, Maria V Popova, Mikhail A Vovk, Alexander V Shvidchenko, Biligma B Tudupova, Victor I Kuular. New Metal-Carbon Heterostructures with Enhanced Relaxivity for MRI Applications. International Journal of Applied Biology and Pharmaceutical Technology. 16 (2025): 02-11.

Lebedev VT, et al., Int J Appl Biol Pharm 2025
DOI:10.26502/ijabpt.202135

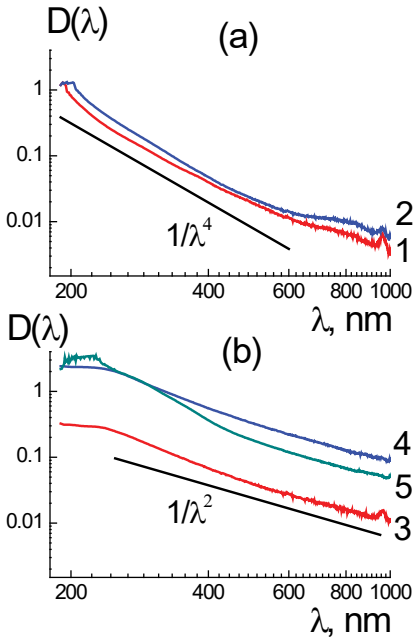

Figure 2: Optical density spectra D(λ) of aqueous dispersions (concentration 0.01% wt.) of diamonds DNDZ+ and DNDZ- (a; 1,2) and fullerenols with Gd, Ho, Fe atoms (b; 3-5). Data (a) for diamonds D(λ) ~ $1/\lambda^4$ demonstrate radiation Rayleigh scattering on particles. For fullerenols (b), other dependence D(λ) ~ $1/\lambda^2$ indicates radiation absorption.

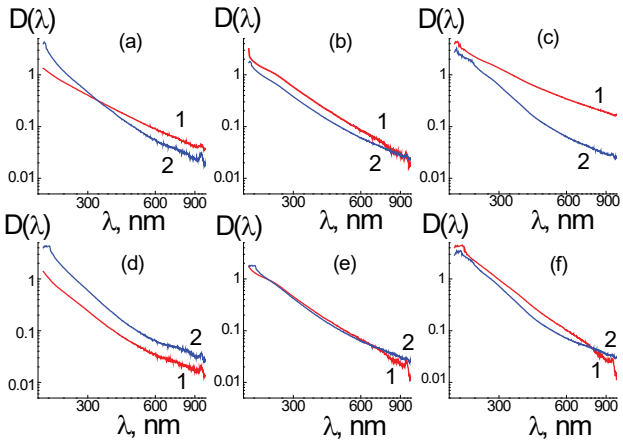

Figure 3: Optical density D(λ) spectra (1) of aqueous dispersions of the complexes of diamonds DNDZ+ (a, b, c) or DNDZ- (d, e, f) with HEF containing Gd (a, d), Ho (b, e), Fe (c, f). Total data (2), $C_1D_1(\lambda)$ + $C_2D_2(\lambda)$ for HEF and DNDZ± components with fractions C_1, C_2 the same as in binary samples are shown.

We controlled complexing in binary aqueous mixtures (20°C) after ultrasonic treatment when compared their electronic spectra with the data for components (Fig.2,3). According to the UV and visible light absorption data, in sonicated binary systems the optical density D(λ) differed from the sum of spectra, $D_{sum}(\lambda) = C_1D_1(\lambda) + C_2D_2(\lambda)$, for HEF and DNDZ± with mass fractions of C_1, C_2 like in mixtures (Fig. 2,3). It is more pronounced in the samples with electronegative HEF and positively charged DNDZ+ particles due to mutual attraction and the contacts of components with charge neutralization (Fig.3).

Due to neutrality, the HEF+DNDZ+ particles were prone to aggregation revealed in the scattering increase and related growth of optical density, $D(\lambda) > D_{sum}(\lambda)$, mostly exceeding the sum $D_{sum}(\lambda)$ of partial spectra (Fig.3a,b,c). However, in binary system with components having the same sign of charges (HEF, DNDZ-) weak or even opposite effect detected, $D(\lambda) < D_{sum}(\lambda)$, as a result of mutual repulsion between the components and/or complexes stabilized by hydrogen bonds and hydrophobic interactions (Fig.3d,e,f).

NMR Experiments

Magnetic relaxation properties of aqueous systems of complexes and components have been studied at ambient temperature (297 K) by NMR (Bruker 500 MHz Avance III spectrometer, NMR Resource Center, St. Petersburg State University). For the samples, the longitudinal and transverse relaxation times of proton spins (T_1, T_2) were found and compared with the data for deionized water (Table 1). To determine the spin–lattice relaxation time T_1 we used the "inversion-recovery" method with pulse sequence 180°–τ–90°. In the measurements of the spin–spin relaxation time T_2 we applied Carr–Purcell multi-pulse sequence 90x°–τ–(180°x–2τ–)*n*. All the relaxation functions were well approximated by a single exponent within the experimental errors. Then to evaluate the contrast properties of substances to water added, we corrected the reciprocal times ($1/T_1$,$1/T_2$) for water contributions ($1/T_{1W}$, $1/T_{2W}$) and calculated the relaxation rates $r_{1,2} = (1/T_{1,2} - 1/T_{1,2W})$ (Fig. 4). Finally, we normalized them to magnetic ion concentrations (C_M) and found the differential relaxivities, $\Delta r = (r_2–r_1)/C_M$ (Tab.1).

Results and Discussion

All the aqueous systems have the relaxation times (T_1, T_2) which are shorter than those in pure water, and a usual relationship $T_2 < T_1$ is kept always (Tab.1). The carbon or metal-carbon additives accelerate the spin relaxation of protons but to different degrees. Comparative to diamonds, the effects of magnetic molecules and especially the complexes with diamonds reach two orders of magnitude that is expressed in high relaxation rates $r_{1,2}$ (Tab.1, Fig. 4). Actually, very small amounts of diamonds DNDZ+, DNDZ- (~3 mg/ml) accelerate a longitudinal relaxation by 24 and 30 % and fasten a transverse relaxation by 87 and 66 %. In fact, it demonstrates the role of diamonds as the active platforms for carrying magnetic molecules.

Citation: Vasily T Lebedev, Natalia P Yevlampieva, Maria V Popova, Mikhail A Vovk, Alexander V Shvidchenko, Biligma B Tudupova, Victor I Kuular. New Metal-Carbon Heterostructures with Enhanced Relaxivity for MRI Applications. International Journal of Applied Biology and Pharmaceutical Technology. 16 (2025): 02-11.

Lebedev VT, et al., Int J Appl Biol Pharm 2025
DOI:10.26502/ijabpt.202135

Magnetic ions by their magnetic fields change proton spins transverse relaxation times T_2 to the greatest extent. The iron containing complex with DNDZ- shows a record rate r_2 being three times greater than that for heterostructures with lanthanides (Fig.4c, data 2). Meanwhile, complexing less affect the longitudinal relaxation rate r_1. The binding of Gd-fullerenols to diamonds causes a strong lowering the rate r_1 (Fig.4a). However, this characteristic is practically not varied when Ho-fullerenols create complexes (Fig.4b). In the case of Fe-fullerenols, the r_1 increase or decrease depends on the platforms (DNDZ-, DNDZ+) (Fig.4c). Ultimately, the efficacies of synthesized new contrast agents for MRI are defined by their differential relaxivities (Δr) evaluated for all the samples (Tab.1). Among fullerenols, the $Ho@C_{82}(OH)_{40}$ molecules demonstrates the greatest magnitude of $\Delta r \sim 7$ $s^{-1}mM^{-1}$, while Gd- and Fe-fullerenols show lower values, $\Delta r \sim 3\text{-}4$ $s^{-1}mM^{-1}$ (Tab.1). Such characteristics for pristine DNDZ+ and DNDZ- diamonds, $\Delta r \sim 2.3x10^{-3}$ and $\sim 1.5x10^{-3}$ $s^{-1}mM^{-1}$, are three orders of magnitude lower, than that for fullerenols (Tab.1). However, complexing Fe-fullerenols provides the great $\Delta r \sim 52$ $s^{-1}mM^{-1}$ for $Fe@C_{60}(OH)_{30}$+DNDZ- structures. This is twice as high as the $\Delta r \sim 24$ and 20 $s^{-1}mM^{-1}$ for $Ho@C_{82}(OH)_{40}$+DNDZ+ and $Gd@C_{82}(OH)_{30}$+DNDZ- (Tab.1). Binding with diamonds improve the contrast power of composites relative to basic indicator Δr_F for fullerenols with Ho, Gd, Fe according to the ratio $\Delta r_{N\pm} = \Delta r/\Delta r_F \sim (2\text{-}3)$, (3-6), (4-12) depending on the platforms. DNDZ+ diamonds provide moderate contrast gains $\Delta r_{N+} \sim 3.3\text{-}3.5$ approximately the same for different magnetic atoms. But DNDZ- diamonds induce very different increments, $\Delta r_{N-} \sim 2.1\text{-}12.1$, which are minimal for Ho containing samples but maximal for complexes with Fe (Fig. 5).

In the case of Gd- and Fe-fullerenols on the DNDZ+ platform, such neutral complexes of oppositely charged components are less effective than the structures with DNDZ- diamonds when the components are like-charged (Fig.5). This can be explained by the greater coagulation of the complexes in the first case and lesser in the second, when the surface of the composite particles is more accessible for water exchange in the volume of the sample. At the same time, the presence of Ho in the samples causes the opposite effect, more pronounced in complexes with DNDZ+ diamonds (Fig. 5). When analyzing the interaction of fullerenols and diamonds, it is important to consider that in an aqueous dispersion, DNDZ- and DNDZ+ particles of average size $d_P \sim 5$ nm with a potential of $\psi \sim 0.05$ V create a high-intensity electric field at the surface, $E \sim 2\psi/d_p \sim 2x10^7$ V/m, acting on the attached fullerenols [9-11]. The effect of the electric field on the vibrational modes of fullerenes was studied in [35], where splitting and activation of vibrational modes in the IR and Raman spectra were established, when the overlap and interaction of closely spaced modes of different symmetries causes their shift to the short-wave region of the spectrum. Under these conditions, high-frequency shell vibrations are transmitted inside the fullerenol to the magnetic ion associated with the carbon shell through charge transfer and electron-phonon interactions. Rapid displacements of the ion through dipole interactions with protons contribute to the acceleration of their spin relaxation, which is observed for the complexes with diamonds DNDZ- and DNDZ+ (Tab.1). In addition to influencing the vibrational modes of fullerenes, the electric fields of diamonds polarize these molecules, causing a displacement of mobile electrons in carbon shells and ions inside them.

The higher relaxivity of Gd-endofullerenes than that of its complexes with low-molecular ligands is explained by the delocalization of unpaired electrons, when the electron spin density is transferred from the paramagnetic atom to the fullerene shell and even beyond it ("spin leakage") [36-38], which was theoretically predicted [39] and confirmed by EPR, ENDOR (electron-nuclear double resonance) and NMR [40]. A similar mechanism is undoubtedly realized for endofullerenes with 3d metals, in particular with iron. However, these structures, which have recently begun to be synthesized [41], have been little studied in comparison with analogs containing lanthanides. In our experiments, the transfer of spin density in fullerenols in the complexes is affected by powerful fields (~$2x10^7$ V/m) of charged diamonds. If the diamond has a negative potential, then the fullerenols on its surface are polarized so that the unpaired electrons on the carbon shells are repelled from the diamond face, shifting to the surface of the shells facing the solution. This contributes to an increase in the relaxation rates of the complexes with Gd^{3+} and Fe^{3+} $r_{2DNDZ-} > r_{2Ful}$ relative to free fullerenol by two (ten) times (Fig.4a,c).

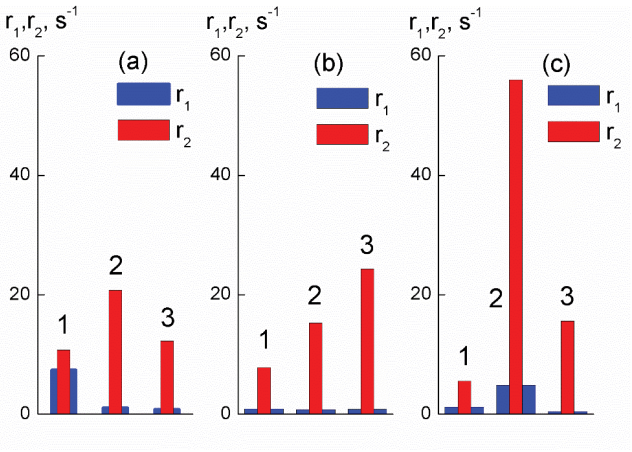

Figure 4: Rates of proton spin longitudinal and transverse relaxation ($r_{1,2}$) in aqueous systems of fullerenols (1) with Gd, Ho, Fe (a,b,c), and the complexes with DNDZ- and DNDZ+ (2,3).

Citation: Vasily T Lebedev, Natalia P Yevlampieva, Maria V Popova, Mikhail A Vovk, Alexander V Shvidchenko, Biligma B Tudupova, Victor I Kuular. New Metal-Carbon Heterostructures with Enhanced Relaxivity for MRI Applications. International Journal of Applied Biology and Pharmaceutical Technology. 16 (2025): 02-11.

Lebedev VT, et al., Int J Appl Biol Pharm 2025
DOI:10.26502/ijabpt.202135

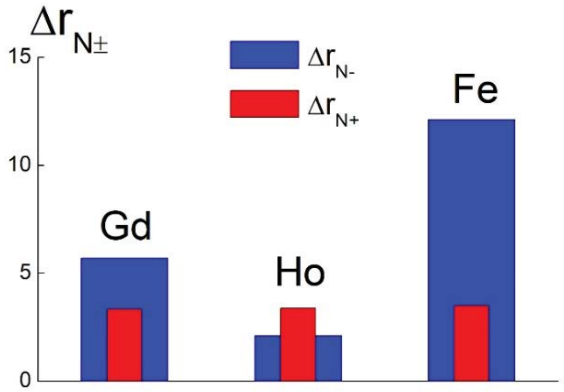

Figure 5: Contrast increments $\Delta r_{N\pm}$ for complexes with DNDZ+ and DNDZ- platforms relative to data for fullerenols containing, Gd, Ho, Fe.

If the diamonds in the complexes are charged positively, then due to the attraction of the carbon shell electrons to the diamond faces, the side of the shell facing the solution is depleted of electrons, and the increase in r_{2DNDZ+} relative to the level for free fullerenols is less than in the first case, $r_{2DNDZ+} < r_{2DNDZ-}$ (Fig.4). It should be noted that the magnetic moments of the Gd^{3+} and Fe^{3+} ions are determined by the spin of the electron system ($S_{Gd} = 7/2$, $S_{Fe} = 5/2$), but for the Ho^{3+} ion, the magnetic moment is determined mainly by the orbital moment of the electrons (L = 6), and the spin $S_{Ho} = 2$ is lower than that of Fe^{3+} [42]. Therefore, for complexes with holmium, the effect of acceleration of transverse relaxation is weaker than for samples with iron with an inverse relationship for relaxation rates $r_{2DNDZ+} > r_{2DNDZ-}$ for complexes with diamonds DNDZ+ and DNDZ-. As for the spin-lattice relaxation, for free fullerenols with Gd^{3+}, Fe^{3+}, Ho^{3+} ions, the relation $r_{1Gd} > r_{1Fe} > r_{1Ho}$ is consistent with the values of the spins, $S_{Gd} > S_{Fe} > S_{Ho}$. In this case, the relaxivities characterize aqueous systems, where fullerenols are prone to aggregation [43]. Molecular self-assembly in mixed solutions of paramagnetic $Gd@C_{82}(OH)_{24-30}$ and diamagnetic $C_{60}(OH)_{24-30}$ fullerenols was studied at room temperature and under the action of a magnetic field (~1 T), which stabilized small supramolecular structures (~20 nm) in such systems in a wide range of concentrations (from dilute to close to the solubility threshold) [43]. Thus, the data on relaxivity for fullerenols with G^{d3+}, Fe^{3+}, Ho^{3+} ions refer to weakly aggregated systems (Tab.1).

In complexes with Gd^{3+}, Fe^{3+}, Ho^{3+} ions, the relationship between relaxivities observed for free fullerenols is disrupted due to differences in the self-organization of complexes in aqueous media, which affects the rates of proton exchange between the complexes and the sample volume. When fullerenols associate with diamonds, the degree of hydrophilicity of their surface changes, and the structure of aggregates of modified diamonds can differ from the original chain (branched) structures of diamond particles (Fig.1) [14,30,31]. This depends on the degree of hydroxylation of fullerenols attached to diamonds. In Fe- and Ho-fullerenols, ~ 50% of the surface is covered with hydroxyls, while in Gd-fullerenols it is only ~ 37%. The addition of less hydrophilic Gd-fullerenols to diamonds causes the formation of aggregates denser than the structures of complexes with Fe- and Ho-fullerenols, which slows down the proton exchange between the complexes with Gd-fullerenols and the aqueous environment, reducing the longitudinal relaxivity relative to the level for free Gd-fullerenols (Fig.4a). At the same time, more hydrophilic Ho-fullerenols do not cause a significant decrease in r_1 values when binding to diamonds, and Fe-fullerenol complexes with DNDZ- diamonds demonstrate a fourfold increase in r_1 (Fig.4b,c).

In fact, already several decades mostly endohedral Gd-fullerenes attract special attention due to the prospects of their application as effective contrast agents in magnetic resonance imaging (MRI) [44]. Relaxivities from 1 to 100 $mM^{-1}s^{-1}$ in various fields are known for the derivatives of $Gd@C_{60}$ and $Gd@C_{82}$ [45,46]. In this regard, the nature of paramagnetic relaxation phenomena caused by these objects and their derivatives, in particular, fullerenols in aqueous media [47], where they show much higher relaxivities than clinically used Gd^{3+} chelates, as well as gadolinium compounds with metals [44,48], is being studied. Traditional contrast agents mainly contain paramagnetic gadolinium ions with high functional characteristics (7 unpaired electrons, large magnetic moment, and long electron spin relaxation time of ~ 10^{-9} s), but concerns remain regarding the toxicity of such agents [48,49]. In this regard, endohedral structures are preferable because they firmly hold heavy metal atoms in carbon shells. However, when studying fullerenols $Gd@C_{60}(OH)x$ ($x \approx 27$), it was found [47] that their relaxivity changes with pH due to aggregation, which depends on pH. In the tested solutions, the spin relaxation rates of ^{17}O and ^{1}H were measured by varying the temperature and magnetic field, and then the aggregation was eliminated by adding sodium phosphate [47]. In the initially aggregated solutions, the ^{17}O $1/T_2$ values were several times higher than $1/T_1$ due to the confinement of water in the spaces between the aggregates during its active exchange with the main water mass, which accelerated the spin-spin relaxation. After the disintegration of the aggregates, individual fullerenols demonstrated relaxivities $1/T_2 > 1/T_1$, which differed little and were determined by the mechanisms of proton exchange at the hydroxyls and water adsorbed on the fullerenols with the main water volume (inner and outer spheres) [47].

Thus, it has been established that near centers with paramagnetic ions, protons in water molecules follow a relaxation behavior, when the longitudinal and transverse

Citation: Vasily T Lebedev, Natalia P Yevlampieva, Maria V Popova, Mikhail A Vovk, Alexander V Shvidchenko, Biligma B Tudupova, Victor I Kuular. New Metal-Carbon Heterostructures with Enhanced Relaxivity for MRI Applications. International Journal of Applied Biology and Pharmaceutical Technology. 16 (2025): 02-11.

Lebedev VT, et al., Int J Appl Biol Pharm 2025
DOI:10.26502/ijabpt.202135

times of spin relaxation of protons in the inner and outer spheres around the center decrease, and the effect depends on the degree of hydration of the paramagnetic center [44-48]. The longitudinal relaxivity of the centers is regulated by a number of parameters (magnetic moments of paramagnetic ions, relaxation times of their electron spin, the rate of rotational relaxation of the centers and the residence times of water molecules near them and their diffusion rates, which affect the contribution of the outer sphere). With regard to transverse relaxivity in strong magnetic fields, the interaction of the nuclear spin with the average electron spin at a certain temperature (the Curie mechanism) is significant [50]. Important factors determining the contribution of the inner sphere to the longitudinal relaxivity are the number of exchanged water molecules directly associated with the paramagnetic center and the residence time of water molecules near it.

In these experiments, a large number of hydroxyls (30; 40) in fullerenol and a comparable number of OH or COOH groups in diamond participate in the proton exchange in the inner sphere in contact with a water monolayer on the surface of these particles (outer sphere). For a fullerenol molecule with a surface area of ~ 6 nm^2, the outer sphere includes ~ 100 H_2O molecules, while for diamond it is an order of magnitude larger. Taking into account the proton migration mechanism according to Grotthuss, the proton residence time in the outer sphere will be ~ 1.5 ps (300 K) [51]. Thus, the high relaxivity of fullerenols with large magnetic moments of ions and complexes of fullerenols with diamonds is ensured by the rapid exchange of protons in the outer sphere and between it and the inner sphere. In complexes, the relaxivity is increased by placing fullerenols on the surface of diamonds, which inhibits the rotation of fullerenols. In their free state, the rotational relaxation time is $\tau_R = 4\pi R_{FH}^3 \eta / 3k_B T \sim 1x10^{-9}$ s, where R_{FH} ~ 1 nm is the hydrodynamic radius of the molecule, η is the viscosity of water, k_B is the Boltzmann constant, T = 300 K is the temperature. For a diamond particle with attached fullerenols, due to its large radius (~ 6 nm), the time $\tau_{RD} \sim 3x10^{-8}$ s is extended by more than an order of magnitude. When using diamond platforms to accommodate magnetic fullerenols, an important factor in increasing relaxivity is the strong ability of diamonds to order into branched chain aggregates, when nanoscale water diffusion channels are created along diamond faces [14,30]. It is known that in thin capillaries, water diffusion is accelerated by several orders of magnitude relative to water in a large volume [52]. In this case, due to this, a rapid proton exchange is realized between the sample volume and the aggregates of complexes, in which a high concentration of magnetic ions accelerates the spin relaxation of protons, and as a result, the relaxivity of the complexes is significantly increased in comparison with free fullerenols in solutions.

The results obtained have shown for the first time the key role of diamond platforms in increasing the contrast properties of magnetic fullerenols with an effect of up to one order of magnitude when they are associated with diamonds. In this way, the desired fine dispersion of fullerenols is achieved and their interaction with the surrounding water is maximized. Meanwhile, hydrophilic fullerenols and other derivatives of endofullerenes are usually highly clustered in aqueous media, and this can weaken their relaxivity [53, 54]. In addition, the most important advantage of new heterostructures is the reliable isolation of magnetic atoms in strong carbon shells of fullerenes from the biological environment [55]. Therefore, such preparations can serve as safe agents for MRI [56], in contrast to traditionally used organometallic structures (phthalocyanines, chelates with magnetic atoms), which are not sufficiently resistant to the chemical effects of biological environments and create risks of intoxication of the body with heavy elements. Overall, the results contribute to the knowledge of magneto-relaxation properties of endohedral structures [57-59] with encapsulated metal atoms, which transfer electrons to carbon cages and can probably magnetize them, depending on their association with diamonds. The significant enhancement of fullerenols' relaxivity observed for the first time due to complexation with diamonds is useful for expanding the scientific basis for theranostic preparations design.

Conclusion

Possibilities of increasing the efficiency of contrast agents for MRI were found using the placement of fullerenols with lanthanides and iron on platforms of detonation nanodiamonds with positive and negative potentials. The experiments proved that the design of heterostructures allowed to enhance the useful effect by an order of magnitude compared to the initial fullerenols. On diamond platforms, a fine dispersion of fullerenols was achieved, when their surface became well accessible for intensive fast water exchange in the sample volume. Therefore, the effect of magnetic atoms enclosed in carbon shells on the spins of water protons was sharply activated. As a result of fullerenols complexing with diamonds, the transverse spin relaxation of protons became significantly accelerated, while the longitudinal relaxation changed only moderately. Thus, the difference in rates gave a gain of up to one order of magnitude, which significantly increases the magneto-relaxation characteristics of the complexes compared to the initial fullerenols. The use of diamond platforms for the placement of magnetic fullerenols opens up new prospects for the development and application of high-contrast agents for MRI with lower concentrations of heavy atoms and minimal risks of associated intoxication due to their strong retention inside fullerenes.

Citation: Vasily T Lebedev, Natalia P Yevlampieva, Maria V Popova, Mikhail A Vovk, Alexander V Shvidchenko, Biligma B Tudupova, Victor I Kuular. New Metal-Carbon Heterostructures with Enhanced Relaxivity for MRI Applications. International Journal of Applied Biology and Pharmaceutical Technology. 16 (2025): 02-11.

Lebedev VT, et al., Int J Appl Biol Pharm 2025
DOI:10.26502/ijabpt.202135

Acknowledgements

This work is supported by the Russian Science Foundation (grant № 25-45-01024). Authors thank the NMR centre of the Saint-Petersburg State University for the delivered ability to perform the experiments and technical help.

References

1. F Chen, EB Ehlerding, W Cai. J Nucl Med 55 (2014): 1919–1922.
2. SM Hosseini, J Mohammadnejad, R Najafi-Taher, Z et al. Multifunctional Carbon-Based Nanoparticles: Theranostic Applications in Cancer Therapy and Diagnosis. *ACS Appl. Bio Mater* 4 (2023): 1323–1338.
3. A. Coene, J. Leliaert, Magnetic nanoparticles in theranostic applications. *J. Appl. Phys* 131 (2022): 160902.
4. B Carrese, G Sanità, A Lamberti. Nanoparticles Design for Theranostic Approach in Cancer Disease. Cancers 14 (2022): 4654.
5. Functionalized Magnetic Nanoparticles for Theranostic Applications. M. Pandey, K. Deshmukh, C. M. Hussain (Eds.). Scrivener Publishing LLC 564 (2025).
6. SE Sandler, B Fellows, O Thompson Mefford. Best Practices for Characterization of Magnetic Nanoparticles for Biomedical Applications. *Anal. Chem* 91 (2019): 14159–14169.
7. D Ho, C-H Katherine Wang, E Kai-Hua Chow. Nanodiamonds: The intersection of nanotechnology, drug development, and personalized medicine. Science Advances 1 (2015): e1500439-e1500439.
8. MI Kanyuk. Use of nanodiamonds in biomedicine. Biotechnologia Acta 8 (2015): 1-25.
9. Vul AY, Dideikin AT, Aleksenskiy AE, et al. Detonation nanodiamonds. In Synthesis, Properties and Applications;Williams, O.A., Ed.; Nanodiamond, RSC Nanoscience and Nanotechnology; RSC Publishing: Cardiff, UK (2014).
10. Piotrovskiy LB, Nikolaev DN, Shenderova OA. Biomedical Applications of Nanodiamonds: Reality and Perspectives. In Detonation Nanodiamonds. Science and Applications; Vul AY, Shenderova OA, Eds.; Pan Stanford Publishing: Danvers, MA, USA (2014): 267–320.
11. Aleksenskii AE. Thechnology of preparation of detonation nanodiamond. In Detonation Nanodiamonds. Science and Applications; Vul AY, Shenderova OA, Eds.; Pan Stanford Publishing: Danvers, MA, USA (2014): 37–72.
12. Aleksenskii A, Bleuel M, Bosak A, et al. Clustering of Diamond Nanoparticles, Fluorination and Efficiency of Slow Neutron Reflectors. Nanomaterials 11 (2021): 1945.
13. A Ya Vul, ED Eidelman, AE Aleksenskiy, et al. Transition sol-gel in nanodiamond hydrosols. Carbon 114 (2017): 242-249.
14. V Lebedev, Yu Kulvelis, A Kuklin, A Vul. Neutron Study of Multilevel Structures of Diamond Gels. Condens. Matter 1 (2016): 1-9.
15. O Bolshakova, V Lebedev, E Mikhailova, et al. Fullerenes on a Nanodiamond Platform Demonstrate Antibacterial Activity with Low Cytotoxicity. Pharmaceutics 15 (2023): 1-20.
16. S Chauhan, N Jain, U Nagaich. Nanodiamonds with powerful ability for drug delivery and biomedical applications: Recent updates on in vivo study and patents. Journal of Pharmaceutical Analysis 10 (2020): 1-12.
17. O Bolshakova, V Lebedev, E Mikhailova, et al. Fullerenes on a Nanodiamond Platform Demonstrate Antibacterial Activity with Low Cytotoxicity. Pharmaceutics 15 (2023): 1984.
18. VT Lebedev, NA Charykov, OS. Shemchuk, et al. Endometallofullerenes and their derivatives: Synthesis, Physicochemical Properties, and Perspective Application in Biomedicine. Colloids and Surfaces B: Biointerfaces 222 (2023): 113133.
19. LM Manus, DJ Mastarone, EA Waters, et al. Gd (III)-nanodiamond conjugates for MRI contrast enhancement. Nano Lett 10 (2010): 484–489.
20. AM Panich, M Salti, SD Goren, et al. Gd (III)-Grafted Detonation Nanodiamonds for MRI Contrast Enhancement. J. Phys. Chem. *C* 123 (2019): 2627–2631.
21. VP Sedov, AA Szhogina, MV Suyasova, et al. Method of obtaining water soluble hydroxylated endometallofullerenes of lanthanides. Patent Rus. Ru 2659972 C1. Reg. 04.07 (2018).
22. Sedov VP, Szhogina AA, Suyasova MV, et al. Method for obtaining endofullerenes of 3d metals. Patent Rus. Ru 2664133 C1. Reg. 15.08 (2018).
23. V Yu Dolmatov. Detonation-synthesis nanodiamonds: synthesis, structure, properties and applications. Russian Chemical Reviews 76 (2007): 339–360.
24. Aleksenskii AE. Thechnology of preparation of detonation nanodiamond. In Detonation Nanodiamonds. Science and Applications; Vul, A.Y., Shenderova, O.A., Eds.; Pan Stanford Publishing: Danvers, MA, USA (2014): 37–72.

Lebedev VT, et al., Int J Appl Biol Pharm 2025
DOI:10.26502/ijabpt.202135

25. Vul A Ya, Dideikin AT, Aleksenskiy AE, et al. Detonation nanodiamonds. Synthesis, properties and applications, in: *Nanodiamond*; Williams, O.A., Ed.; RSC Nanoscience and Nanotechnology: Cardiff (2014): 27-48.

26. Williams O, Hees J, Dieker C, et al. Size-dependent reactivity of diamond nanoparticles. ACS Nano 4 (2010): 4824-4830.

27. Yu S Grushko, VS Kozlov, TO Artamonova, et al. Concentrating of Higher Metallofullerenes. // Fullerenes, Nanotubes, and Carbon Nanostructures 20 (2012): 351–353.

28. VM Cherepanov, VT Lebedev, AA Borisenkova, et al. Valency and coordination of iron with carbon in the structures based on fullerene C_{60}according to the data of gamma-resonance spectroscopy and EXAFS. // Crystallography 65 (2020): 420-424.

29. Vasily T Lebedev, Mikhail V Remizov, Valery S Kozlov, et al. Structuring of Endofullerenols with Lanthanides in Aqueous Solutions. In “Emerging Sustainable Nanomaterials for Biomedical Applications” (Seema Garg, Amrish Chandra, Suresh Sagadevan Eds.) Springer: Springer Nature Switzerland AG (2024).

30. A Ya Vul, ED Eidelman, AE Aleksenskiy, et al. Transition sol-gel in nanodiamond hydrosols. Carbon 114 (2017): 42-249.

31. Yu V Kulvelis, AV Shvidchenko, AE Aleksenskii, et al. Vul. Stabilization of detonation nanodiamonds hydrosol in physiological media with poly(vinylpyrrolidone). Diamond & Related Materials 87 (2018): 78–89.

32. Yu I Neronov, DD Kosenkov. Development of an NMR Relaxometer for Determining Magnetization Dynamics of Water Protons in Living Tissues and Its Use for Evaluating Age-Related Changes. Technical Physics 64 (2019): 1055–1059.

33. E Rtirhej. Proton spin relaxation by paramagnetic molecular oxygen. Canadian Journal of Chemistry 43 (1965): 1130-1138.

34. S Alcicek, P Put, A Kubrak, et al. Zero- to low-field relaxometry of chemical and biological fluids. Communications Chemistry 165 (2023): 1-9.

35. AV Tuchin. Rearrangement and activation of oscillatory modes of fullerene C60 and C70 in an electric field. Condensed matter and interface boundaries 16 (2014): 323-33.

36. VK Koltover. Endofullerenes: from chemical physics to basic elements for nanotechnology and nanomedicine. Rus. Chem. J. (Journal of the Russian Chemical Society named after D.I. Mendeleyev) 2 (2009): 79-85.

37. Koltover VK. Spin-leakage of the fullerene shell of endometallofullerenes: EPR, ENDOR and NMR evidences. Carbon 42 (2004): 1179-1183

38. Koltover VK. Endohedral fullerenes: from chemical physics to nano- technology and nanomedicine In: Progress in Fullerene Research. Ed. M. Lang. New York: Nova Science Publ (2007): 199—233.

39. Buchachenko AL. J Phys. Chem. B 105 (2001): 5839-5846.

40. Koltover VK, Parnyuk TA, Bubnov VP, et al. Dokl. RAS 384 (2002): 28-30.

41. Sedov VP, Szhogina AA, Suyasova MV, et al. Method for obtaining endofullerenes of 3d metals. Application: 2017108883, 16.03.2017. Effective date for property rights: 16.03.2017. Registration date: 15.08.2018. Proprietor(s): Federalnoe gosudarstvennoe byudzhetnoe uchrezhdenie "Peterburgskij institut yadernoj fiziki im. B.P. Konstantinova" (FGBU "PIYAF") (RU) 23 (2018): 1-13.

42. NV Kudrevatykh, AS Volegov. Magnetism of rare earth metals and their intermetallic compounds. Ekaterinburg, Ural University Publishing House 198 (2015): 27-29.

43. VT Lebedev, VV Runov, AA Szhogina, et al. Nanosyst. Phys. Chem. Math 7 (2016): 1–7.

44. A Rodríguez-Galván, M Rivera, P García-López, et al. Gadolinium-containing carbon nanomaterials for magnetic resonance imaging: Trends and challenges. J. Cell. Mol. Med 24 (2020): 3779-3794.

45. P Anilkumar, F Lu, L Cao, et al. Fullerenes for Applications in Biology and Medicine. Current Medicinal Chemistry 18 (2011): 2045-2059.

46. B Sitharaman, LA Tran, QP Pham, et al. Gadofullerenes as nanoscale magnetic labels for cellular MRI. Contrast Media & Molecular Imaging 3 (2007): 139-146.

47. S Laus, B Sitharaman, É Tóth, et al. Understanding Paramagnetic Relaxation Phenomena for Water-Soluble Gadofullerenes. J. Phys. Chem. *C* 111 (2007): 5633–5639.

48. Venu AC, Nasser Din R, Rudszuck T, et al. NMR Relaxivities of Paramagnetic Lanthanide-Containing Polyoxometalates. Molecules 26 (2021): 7481.

49. Rogosnitzky M, Branch S. Gadolinium-based contrast agent toxicity: A review of known and proposed mechanisms. BioMetals 29 (2016): 365–376.

50. Peters JA, Huskens J, Raber DJ. Lanthanide induced shifts and relaxation rate enhancements. Prog. Nucl. Magn. Reson. Spectrosc 28 (1996): 283–350.

Citation: Vasily T Lebedev, Natalia P Yevlampieva, Maria V Popova, Mikhail A Vovk, Alexander V Shvidchenko, Biligma B Tudupova, Victor I Kuular. New Metal-Carbon Heterostructures with Enhanced Relaxivity for MRI Applications. International Journal of Applied Biology and Pharmaceutical Technology. 16 (2025): 02-11.

Lebedev VT, et al., Int J Appl Biol Pharm 2025
DOI:10.26502/ijabpt.202135

51. SA Fischer, BI Dunlap, D Gunlycke. Correlated dynamics in aqueous proton diffusion. Chem. Sci 9 (2018): 7126.

52. Ryzhkin, I.A.; Ryzhkin, M. I.; Kashin, A. M.; et al. High proton conductivity state of water in nanoporous materials. Europhysics Letters **2019**, 126(3), 36003-36010.

53. M. V. Suyasova, V. T. Lebedev, V. P. Sedov, et al. Proton Spin Relaxation in Aqueous Solutions of Self-assembling Gadolinium Endofullerenols. Appl. Magnetic Resonance 2019, 50,1163–1175.

54. V. T. Lebedev, Yu. V. Kulvelis, A. S. et al. Mechanisms of supramolecular ordering of water-soluble derivatives of fullerenes in aqueous media, Fullerenes, Nanotubes and Carbon Nanostructures 2020, 28,1, 30-39.

55. K. Ghiassi, M. M. Olmstead, A. Balch. Gadolinium-containing endohedral fullerenes: Structures and function as magnetic resonance imaging (MRI) agents. Dalton Transactions 2014 43(20),7346-7358.

56. R.D. Bolskar. Gadolinium Endohedral Metallofullerene-Based MRI Contrast Agents. In: Cataldo F., Da Ros T. (eds) Medicinal Chemistry and Pharmacological Potential of Fullerenes and Carbon Nanotubes. Carbon Materials: Chemistry and Physics, vol 1. Springer, Dordrecht. 2008, P. 157-180.

57. G. Magnin, P. Bissel, R. McAlister Council-Troche, Zю Zhou, M. Ehrich. Studies Exploring the Interaction of the Organophosphorus Compound Paraoxon with Fullerenes. ACS Omega 2019, 4, 18663−18667.

58. J-P. Zheng, Q-L Liu, M-M Zhen, et al. Multifunctional imaging probe based on gadofulleride nanoplatform. Nanoscale, 2012, 4, 3669.

S Laurent, C Henoumont, D Stanicki, et al. Paramagnetic Gadolinium Complexes. In MRI Contrast Agents, Nanotheranostics, Springer Singapore: 2017, p. 23-53.

Citation: Vasily T Lebedev, Natalia P Yevlampieva, Maria V Popova, Mikhail A Vovk, Alexander V Shvidchenko, Biligma B Tudupova, Victor I Kuular. New Metal-Carbon Heterostructures with Enhanced Relaxivity for MRI Applications. International Journal of Applied Biology and Pharmaceutical Technology. 16 (2025): 02-11.